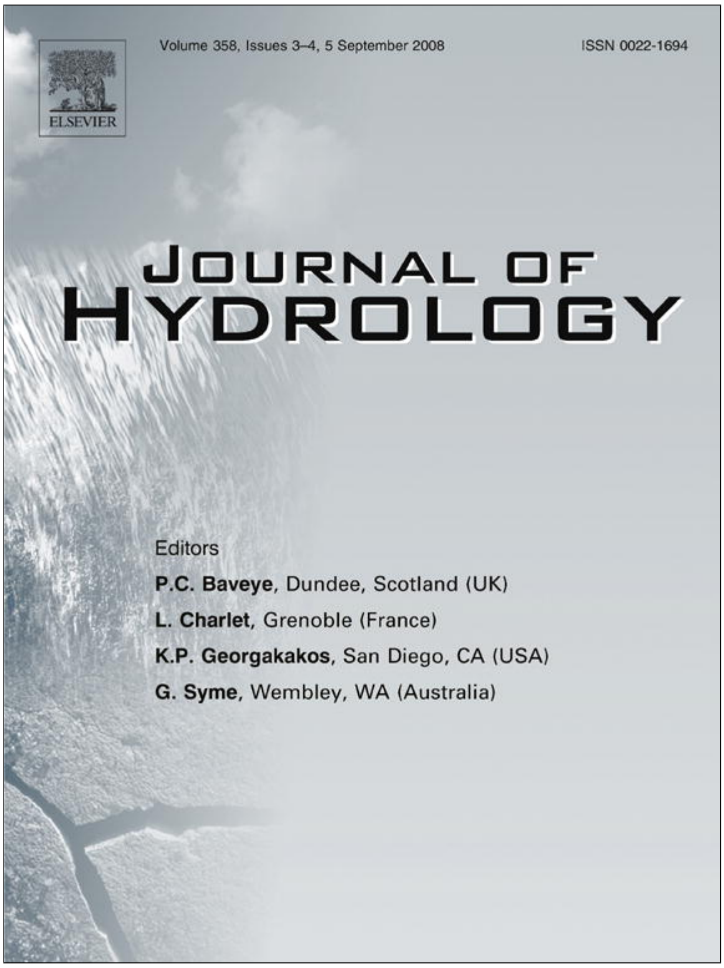
Volume 358, Issues 3–4, 5 September 2008
ISSN 0022-1694
ELSEVIER
JOURNAL OF
HYDROLOGY
Editors
P.C. Baveye, Dundee, Scotland (UK)
L. Charlet, Grenoble (France)
K.P. Georgakakos, San Diego, CA (USA)
G. Syme, Wembley, WA (Australia)

Journal of Hydrology (2008) **358**, 145–158

available at www.sciencedirect.com

ScienceDirect

journal homepage: www.elsevier.com/locate/jhydrol

Development and properties of 0.25-degree gridded evapotranspiration data fields of China for hydrological studies

Axel Thomas *

Institute of Geography, Justus Liebig University, Senckenbergstr. 1, 34390 GieBen, Germany

Received 12 July 2007; received in revised form 26 February 2008; accepted 12 May 2008

KEYWORDS
Reference evapotranspiration;
China;
Gridded data;
Spatial distribution;
Run-off;
Interpolation

Summary Construction and spatial and temporal properties for a 0.25° resolution gridded data set of monthly Penman–Monteith reference evapotranspiration estimates over the territory of the PR China (including Tibet) and adjacent areas (15°N–55°N, 65°E–135°E) for the period 1951–1990 are described. To account for the interaction between climate and the rugged topography of the study area the REGEOTOP procedure was used to incorporate the effects of relief forms into the interpolation.

Evapotranspiration rates over much of China show a range of values (annual rates from 550–2300 mm) and variability comparable to precipitation. Monthly evapotranspiration rates are distributed more evenly over the year than precipitation, are out of phase with the summer precipitation peak and in some cases may reach winter rates comparable to those in summer. Hydrological studies based on idealized regular seasonal variation of evapotranspiration may contain considerable errors due to inherent seasonal fluctuations as compared to precipitation.

High resolution gridded PET data that account for the influence of topography on climate are required to resolve the spatial heterogeneity of topography and land use in order to allow precise estimates of actual evapotranspiration and run-off. The spatial distribution of runoff appears to have remained fairly constant over most of China during 1951–1990 which stands in contrast to the anticipated increase in hydrological activity under global warming conditions.

* Tel.: +49 641 36210; fax: +49 641 36209.
E-mail addresses: axel.thomas@geogr.uni-giessen.de, a.thomas@geo.uni-mainz.de

0022-1694/$ - see front matter
doi:10.1016/j.jhydrol.2008.05.034

Introduction

Evapotranspiration (ET) is a central element of the hydrological cycle, governing the moisture transfer to the atmosphere and thereby influencing fundamental properties of terrestrial ecosystems such as runoff, soil moisture and plant growth. However, basic interactions between atmosphere, soil and plants are still under discussion (e.g. Brutsaert and Parlange, 1998; Golubev et al., 2001; Ohmura and Wild, 2002; Peterson et al., 1995; Roderick and Farquhar, 2002) and even basic properties such as annual totals and variability of ET are not precisely known for many regions of the world. ET is of particular concern in Asia where the convection above the Tibetan Plateau and hence the transfer of latent energy to the atmosphere directly influences the intensity of the Asian monsoon system. Changes in the monsoon circulation affect the livelihood of a major part of the population of Earth. In this respect the uncertainty of the amount and spatio-temporal distribution of ET over East Asia has to be considered a major drawback for hydrological and environmental studies.

As ET cannot be measured directly without considerable effort, it has to be estimated from meteorological data and/or using hydrological methods. The Penman–Monteith (PM) equation has emerged as the de-facto standard to calculate potential ET (PET) with the help of meteorological data. PM PET estimates represent a climatological standard that depends only on atmospheric conditions (assuming reference land surface conditions) and is particularly suitable to compare evaporative conditions over large regions experiencing different climates. Here the implementation of FAO-56 (Allen et al., 1998) is used to calculate PET in the specific form of 'reference' ET (ET0) which assumes fixed values for crop surface resistance, albedo and crop height of 70 sm^{-1}, 0.23 and 0.12 m, respectively.

The PM equation however requires data that are taken routinely only at major observatories (solar radiation, temperature, relative humidity, wind speed) and thus are only available in limited numbers. To estimate ET with a limited set of meteorological data a number of empirical procedures have been developed such as those of Thornthwaite (1948) or Priestley and Taylor (1972) that give less reliable results, particularly in humid climates. Even though this was already noted by Thornthwaite (1951) several recent studies that deal with hydrological or ecological applications rely on temperature-based ET estimates (e.g. Döll et al., 2003; Hagg et al., 2007; Legates and Mather, 1992; Legates and McCabe, 2005; Milly, 1994). The same applies to studies of vegetation distribution and hydrological properties of China (Ma and Fu, 2003; Yue et al., 2005, 2007; Zheng, 1996) thereby compromising the accuracy of their results. Several studies (Garcia et al., 2004; Chen et al., 2005, 2006) have shown that use of either Thornthwaite or Priestley–Taylor formulations underestimate PET considerably.

Recently a large ET station data base covering the territory of the PR China has been developed (Gao et al., 2006) that partly alleviates the data deficiency problem. In a largely mountainous country (local elevation differences within short distances often >500 m) such as China the spatial variation of any climatic element however cannot adequately be described by point data. In order to calculate gridded data that describes the actual variation with topography ET interpolation procedures not only need to account for any dependence of ET to elevation, but also for the much more complicated interaction between topography and cloud formation that in turn determines the solar energy available for ET. Due to the largely mountainous nature of China any spatial representation of ET has to offer at least a resolution of ~25 km to represent the typical topographic features of deep river valleys and intramontane basins that characterize considerable parts of China.

Gridded ET estimates from Global Climate Model (GCM) results lack the resolution that is required to predict the spatial variability that is observed in mountainous terrain (e.g., Calanca et al., 2006). This implies that observed gridded ET data are required as a means to calibrate the results from GCM experiments rather than be substituted by GCM results themselves.

In general more stations measure air temperature than stations that measure sunshine duration or wind speeds. To incorporate all available stations in an ET estimation scheme it appears tempting to first interpolate all input variables into separate grids and then to calculate ET from the gridded input data (IC procedure). As a drawback this requires four separate interpolations with interpolation of wind speeds from surface observations being particularly demanding (depending on data density and topography). The IC procedure was used for the IWMI (International Water Management Institute) World Water & Climate Atlas (pers. comm. I. Makin) based on data from New et al. (2002) and high resolution (100 m) grids for a study area in the Loess Plateau in China (McVicar et al., 2007). As individual errors of the interpolation procedures are additive the overall error of IC should be larger than the error of a calculation on station basis (Bechini et al., 2000; Philips and Marks, 1996). Even though Mardikis et al. (2005) found no appreciable difference between gridded ET data interpolated with both methods the large uncertainties in interpolating wind data from a sparse station network with a simple interpolation scheme (Walter et al., 2006) and the difficulty in assessing the cumulative error of the IC method appear to make the IC approach less reliable at the 0.25° resolution discussed here. For studies at the landscape level which require very high resolution grids (100 m or less) the IC approach allows for the direct inclusion of illumination effects on the surface energy balance (McVicar et al., 2007; Vicente-Serrano et al., 2007) and should yield superior results if a physically-based formulation of ET as in the case of McVicar et al. (2007) is used.

To investigate the spatial and temporal distribution of ET over China this study presents monthly ET0 estimates for the period 1961–1990 gridded at 0.25° resolution. ET0 estimates have been interpolated with the REGEOTOP procedure (Thomas and Herzfeld, 2004) that accounts explicitly for the influence of relief forms on climate. Spatial and temporal characteristics of the data related to hydrological modelling are discussed here. To demonstrate the potential of high resolution ET0 grids spatial estimates of the aridity index, runoff and actual evapotranspiration are presented and discussed.

Study area and data

The study area is located between latitudes 15°N–55°N and longitudes 65°E–135°E. With the exception of the polar, subpolar and inner tropical climates all climate zones occur in this region. A further modification occurs through the mostly mountainous topography with elevations ranging from −154 m (Turpan Basin) to 8848 m (Mt. Everest; Chomolongma). The large difference in latitude leads to a pronounced variation in illumination conditions during the year: in South China the minimum and maximum daily sunshine duration are 11 and 13 h while in North China they are 7 and 17 h, respectively. Due to its location at the eastern margin of the Eurasian continent the climate of the eastern part of China is monsoonal with warm and humid summers and temperate, dry winters. Towards the west continental conditions prevail under mostly westerly air masses culminating in the arid Taklamakan desert basin. The Tibetan Plateau with average elevations of 4500 m dominates the southwestern part of the study area (Fig. 1).

A total of 200 stations maintained by the State Meteorological Administration of China were available that allowed to calculate ET0 estimates. Daily ET0 rates were estimated according to the Penman–Monteith procedure as outlined in Allen et al., 1998 and summed to monthly values. The Penman–Monteith approach is regarded as the most accurate method under all climates giving estimates that differ less than ±10% from the actual values (Jensen et al., 1990). After homogeneity analysis based on three independent test methods (Buishand, 1982; Mitchell, 1966; Scueltus, 1969) four stations were excluded. The final station data set consisted of 196 stations covering an elevational range from sea level in southeastern China to 4800 m on the Tibetan Plateau (Fig. 1).

Regionalisation method

Previous approaches to grid climate data over China have relied on direct interpolation procedures (Baker, 1999) or regionalization procedures that take only elevation into account (New et al., 2002; Prieler, 1999). In order to account for the spatial variability imparted on ET0 rates by the particularly rugged topography of China a regionalization procedure is required that does not only include elevation related effects but is also capable of integrating topography related effects such as cloud formation and dissipation on windward and leeward slopes or the effects of air masses repeatedly crossing mountain chains. The REGEOTOP procedure uses multivariate stepwise regression analysis to relate the large scale station distribution and relief forms derived from a digital elevation model to climate data and applies geostatistical techniques to integrate regression residuals for an optimum amount of variance. Grids were calculated for the period 1951–1990 at 0.25° resolution. Prior to 1960, however, only a limited number of stations were operational in China and 1951–1960 grids have a lower quality than 1961–1990 grid. Consequently most of the data used in this study are restricted to gridded monthly ET0 data for the climatic normal 1961–1990. In addition monthly grids of temperature and precipitation (P) at the same resolution were calculated. Details of the method can be found in Thomas and Herzfeld (2004).

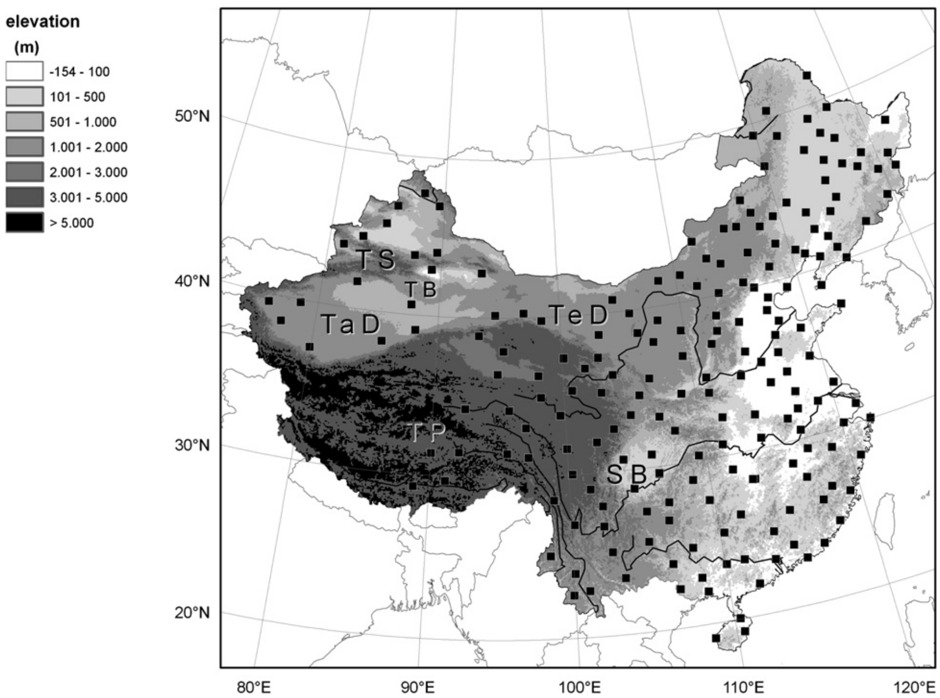

Figure 1 Overview of the study area. Meteorological stations contributing to REGEOTOP ET0 grids are shown as squares. Major Asian rivers are (clockwise from northeast) the Yellow River (Huang He), Yangtze River (Chang Jiang), Pearl River (Xi Jiang), Mekong, Salween, Irrawaddy and the Yalong Tsangpo (the upper reaches of the Brahmaputra in Tibet). TP, TS, TaD, TeD, SB and TB identify the Tibetan Plateau, Tian Shan Mountains, Taklamakan desert, Tengger desert, Sichuan Basin and Turpan Basin, resp.

The regression results indicate that a considerable amount of spatial variance of ET0 rates can already be explained by large scale variation in latitude and elevation which points to the importance of solar radiation to the evaporative processes. In addition relief forms allow small scale variations critical for a high resolution representation of the spatial ET0 distribution in mountainous terrain to be explained. While the effects of exposition-related relief features are to be anticipated, landforms that consist of a series of parallel ridges appear in the regression equation. These may reflect the desiccating effect of repeated lifting of air masses over consecutive mountain chains, described by Fliri (1967) for the European Alps.

Geostatistically interpolated residual fields were added to the fields obtained from the regression analysis, accounting for the variance not explained by the regression model. As large scale variability, such as seasonal variations of solar radiation and topographic effects, have been accounted for by the regression analysis the assessment of monthly residuals may reveal information regarding synoptic climatology. Variogram analysis shows considerable interannual and seasonal variation in spatial cohesion (the range parameter), information content (the sill parameter) and functional relationship (the shape of the variogram) of the residual fields (Fig. 2). In July spatial coherence can be observed to a mean distance of 2050 km while in January this value drops to 1150 km. High summer cohesion appears to reflect the more uniform weather conditions experienced during the summer monsoon, compared to winter when local topographic influences prevail.

The accuracy of the gridded data (Table 1) shows a definite seasonal variation that is thought to reflect the influ-

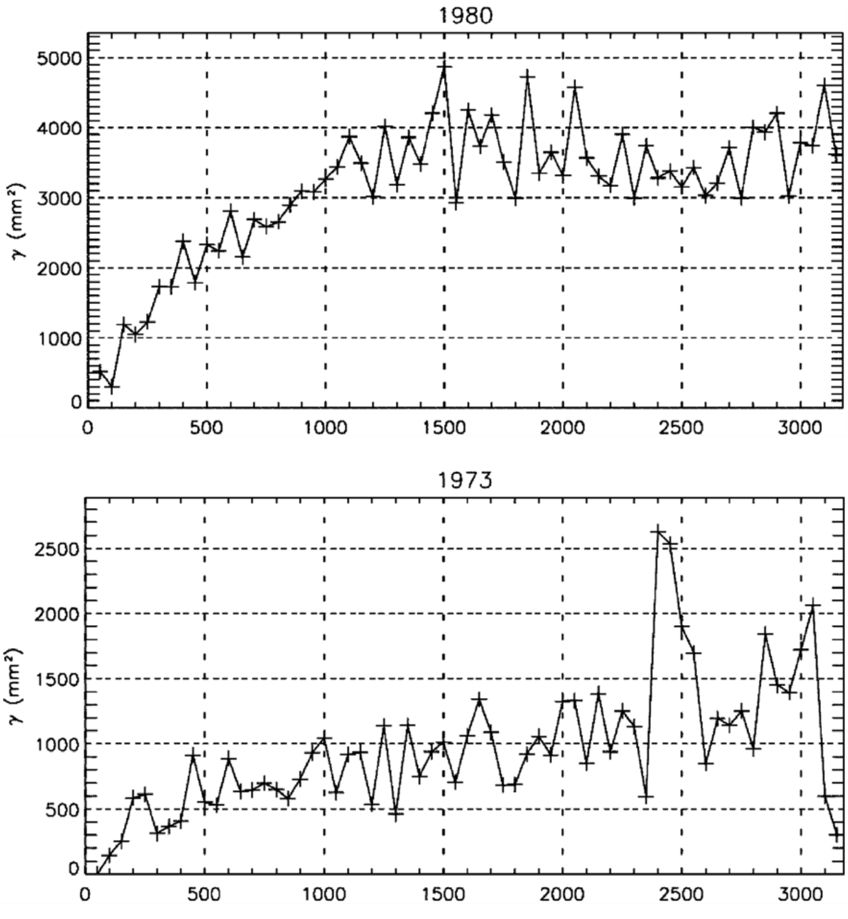

Figure 2 Examples of two contrasting variograms of ET0 residuals for the peak monsoon month July calculated with a lag of 50 km. In 1980 (top) inter-station correlation drops off quickly with distance and reaches a minimum of 1500 km while in 1973 (bottom) information almost linearly drops off but reaches no definitive lower limit within the domain of the study area (3200 km). Note that vertical axes have different scales and hence information content is vastly different.

Table 1 Average rms-values, relative differences (O—C) and correlation coefficients between observed monthly station values and calculated grid values of reference evapotranspiration

	January	February	March	April	May	June	July	August	September	October	November	December
rms (mm)	5.7	6.7	10.6	14.8	20.7	21.4	24.2	24.0	14.4	9.7	8.3	6.3
(O—C) %	5.3	0.1	1.6	3.9	3.9	2.8	0.1	1.9	3.9	6.6	7.6	8.6
R^2	0.959	0.948	0.917	0.895	0.897	0.920	0.915	0.893	0.915	0.928	0.925	0.954

ence of different circulation regimes during the course of the year particularly in the transition months of autumn and in early winter. With O–C-values between 0.1% (February, July) and 8.6% (December) the accuracy lies between the values obtained for *P* and temperature with the REGEOTOP procedure in the same study domain. As the elevation difference between a meteorological station and the single value prescribed for each 25 km resolution grid cell may exceed 2000 m considerable differences are expected.

Results

Long-term monthly and annual totals

The spatial distribution of annual ET0 rates (Fig. 3, top) shows a strong contrast between high rates in western and to a lesser extent southeastern China and low rates in central China. Maximum annual ET0 rates of ~2300 mm are found in the southern Taklamakan desert and rates >2000 mm occur both north and south of the Tian Shan range. The lowest annual rates of 550 mm are estimated for the Sichuan basin. Low ET0 rates would also be expected at high elevations. Even though the effect of topography on ET0 rates is evident through lower ET0 rates in major mountain ranges, annual ET0 rates on the Tibetan Plateau (900–1200 mm) are comparable to those of south central China and parts of northeastern China, both some 3000 m lower.

The spatial distribution of ET0 rates in summer and winter varies considerably. In winter (Fig. 3, center) an almost pure meridional decrease of ET0 rates from the south to the north is observed. The only large scale disturbances are a tongue of low ET0 rates extending southward into the Sichuan Basin (at ~105°E, 35°N) and an extension of higher ET0 rates extending northwards from southwestern China (at ~102°E, 25°N). In winter, ET0 rates of less than 1 mm/month are found in northeastern China, with maximum monthly winter ET0 rates of 140 mm observed in southwestern China (where vast areas experience monthly rates of ~100 mm).

In contrast, summer monthly ET0 rates vary around 100–200 mm and are mainly oriented in an east–west pattern (Fig. 3, bottom). Maximum rates of up to 400 mm are found in the desert of the eastern Taklamakan desert basin and the Tengger desert in western China. Mountain ranges and the Tibetan Plateau act as azonal elements with reduced monthly ET0 rates of <100 mm.

Temporal variability

Only limited information is available concerning interannual variability of ET0 rates. ET0 could be regarded as a conservative climatic element with low variability as solar insolation as the primary energy source of ET is a stable climatic element both in temporal and spatial terms. Fig. 4 (top) however shows that even in winter variability (expressed as the coefficient of variability CV) reaches values >30% of the long term mean over large parts of China. Variability appears to increase at higher elevations reaching a maximum in the mountains of northwest and northeast China. In summer (Fig. 4, bottom) variability decreases slightly over large parts of eastern China (west of 105°E) and northwestern China in relation to the long-term mean (CV values in the range of 10–20%). This is comparable to CV values of July *P* in many parts of this area. Similar to the winter season high variability (CV up to 100%) is found in the mountain ranges east and south of the Tibetan Plateau.

Linear trend rates

Linear trend rates give a generalized idea of change of ET rates over time. Fig. 5 (top) shows that in winter eastern China experiences in general decreasing trends of less than 1 mm/decade (not significant at $P = 95\%$). Increasing ET0 rates of a similar magnitude occur in the mountains surrounding the Tibetan Plateau. An obvious feature is the strong contrast in opposing trends in the mountains of Southwest China. In summer positive trends of up to 5 mm/decade are centered on high-evaporation areas in the western deserts (Fig. 5, bottom). Close by along the border to Mongolia decreasing trends of nearly similar magnitude are observed. Negative trends of up to −2 mm/decade are in general found in eastern China while positive trends of the same magnitude are mostly restricted to western China and the Tibetan Plateau.

Water balance

Water availability expressed in form of the aridity index AI (Budyko, 1974)

$$\mathrm{AI} = P/\mathrm{ET0}$$

gives a first basic idea of hydrological conditions within the study area (Fig. 6). AI > 1 indicates humid conditions where water availability (*P*) exceeds atmospheric water demand (ET0). Humid areas are restricted to regions south of 32°–34°N and east of 102°E and to the extreme southwest border region where AI values vary considerably over short distances and reach values >2.5. In the remaining arid part of China AI values drop to levels as low as 0.01. The AI gradient towards the northwest is smooth and shows no indication of the influence of topography. A comparison with AI based on the period 1951–1980 shows that the position of the transition zone between humid and arid areas (AI = 1) has remained more or less constant (Fig. 6).

Assuming steady state water balance, annual average actual evapotranspiration $\mathrm{ET_a}$ is determined as

$$\mathrm{ET_a} = \mathrm{ET0} \quad \mathrm{ET0} \le P$$

$$\mathrm{ET_a} = P \quad \mathrm{ET0} > P$$

In the first case environmental conditions are energy-limited, in the second case water-limited.

In this study $\mathrm{ET_a}$ is simplified by disregarding water storage (in soils or as snow) and the influence of vegetation and soil properties on ET rates (Donohue et al., 2007). Annual $\mathrm{ET_a}$ (summed from long-term average monthly totals) shows a similar southeast–northwest trend as AI with maximum values of up to 1200 mm in the coastal regions decreasing to less than 100 mm in the western deserts (Fig. 7). Again topography does not appear to contribute to the observed spatial distribution. The transition from water-limited (arid) to energy-limited (humid) environments occurs over a large range of $\mathrm{ET_a}$ values (200–1200 mm/a).

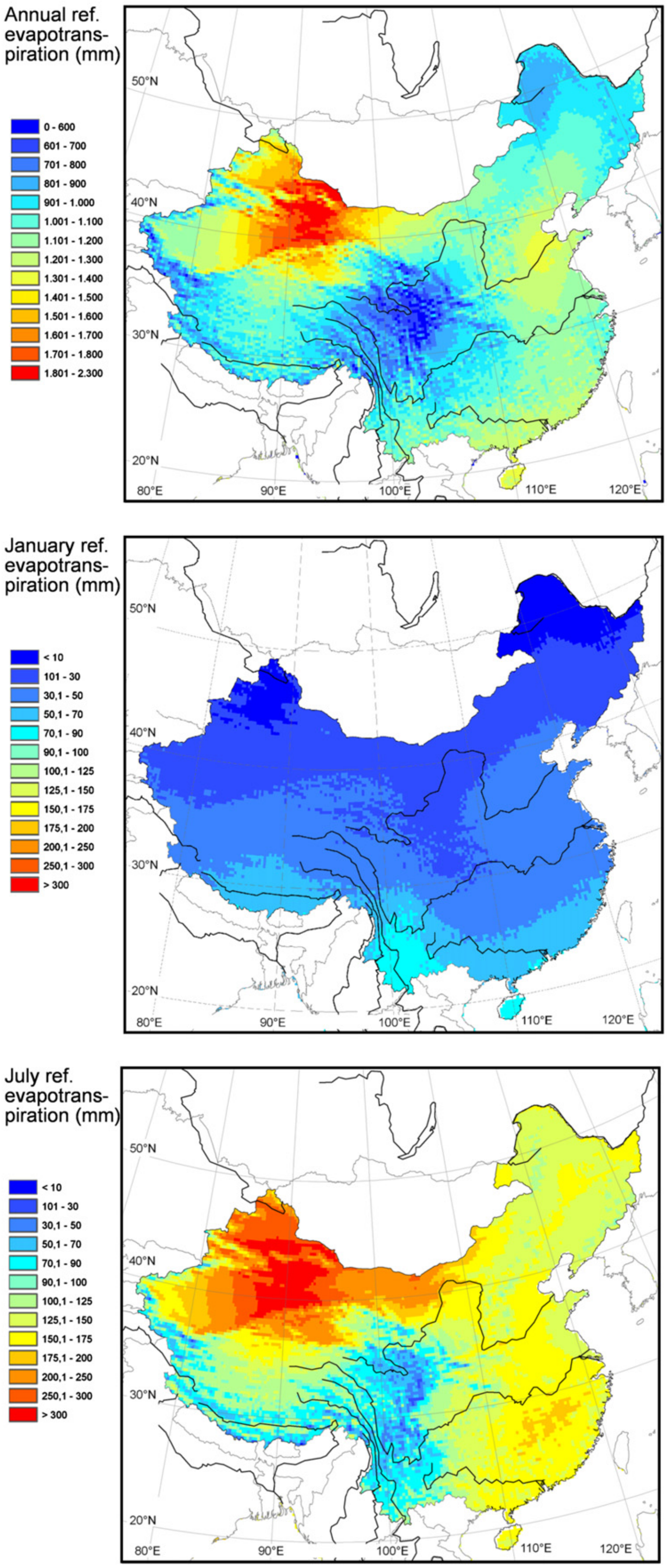

Figure 3 Mean annual, January and July (from top to bottom, resp.) Penman—Monteith reference evapotranspiration (1961—1990).

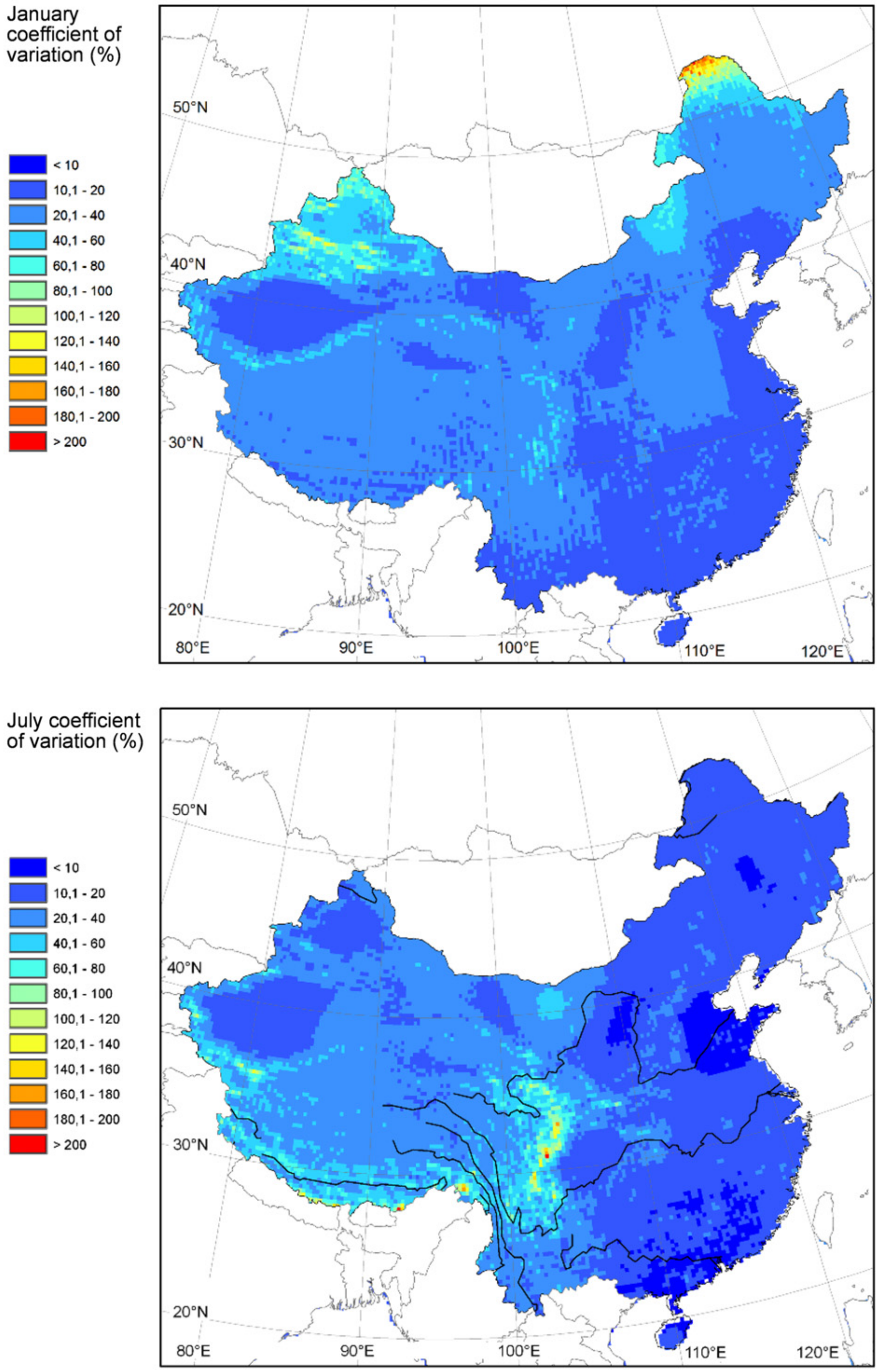

Figure 4 January (top) and July (bottom) Penman—Monteith reference evapotranspiration coefficient of variation (1961—1990).

ET_a and P constitute the two major input variables in the water balance equation (assuming steady state, Donohue et al., 2007)

$$Q = P - ET_a$$

with Q as runoff. Annual values of Q (again calculated on a monthly basis with long-term average monthly totals and summed to an annual value) divide China in two roughly equal parts along a diagonal transition line (Fig. 8). With the exception of the extreme northwest no runoff occurs in the western part of China. Within the humid area defined by $AI > 1$ Q exceeds values of 400 mm/a. Maximum Q ($\sim$2500 mm/a) occurs in the regions of maximum summer P along the South China coast and on isolated inland mountain slopes. Basing the calculation of Q on annual values or substituting ET_a with ET0 considerably alters the spatial distribution towards more arid conditions as the asynchronous annual variation of ET_a and Q is not taken into account.

If Q is displayed in relation to P (runoff fraction, Fig. 9) maximum values >0.8 are found in the headwater regions

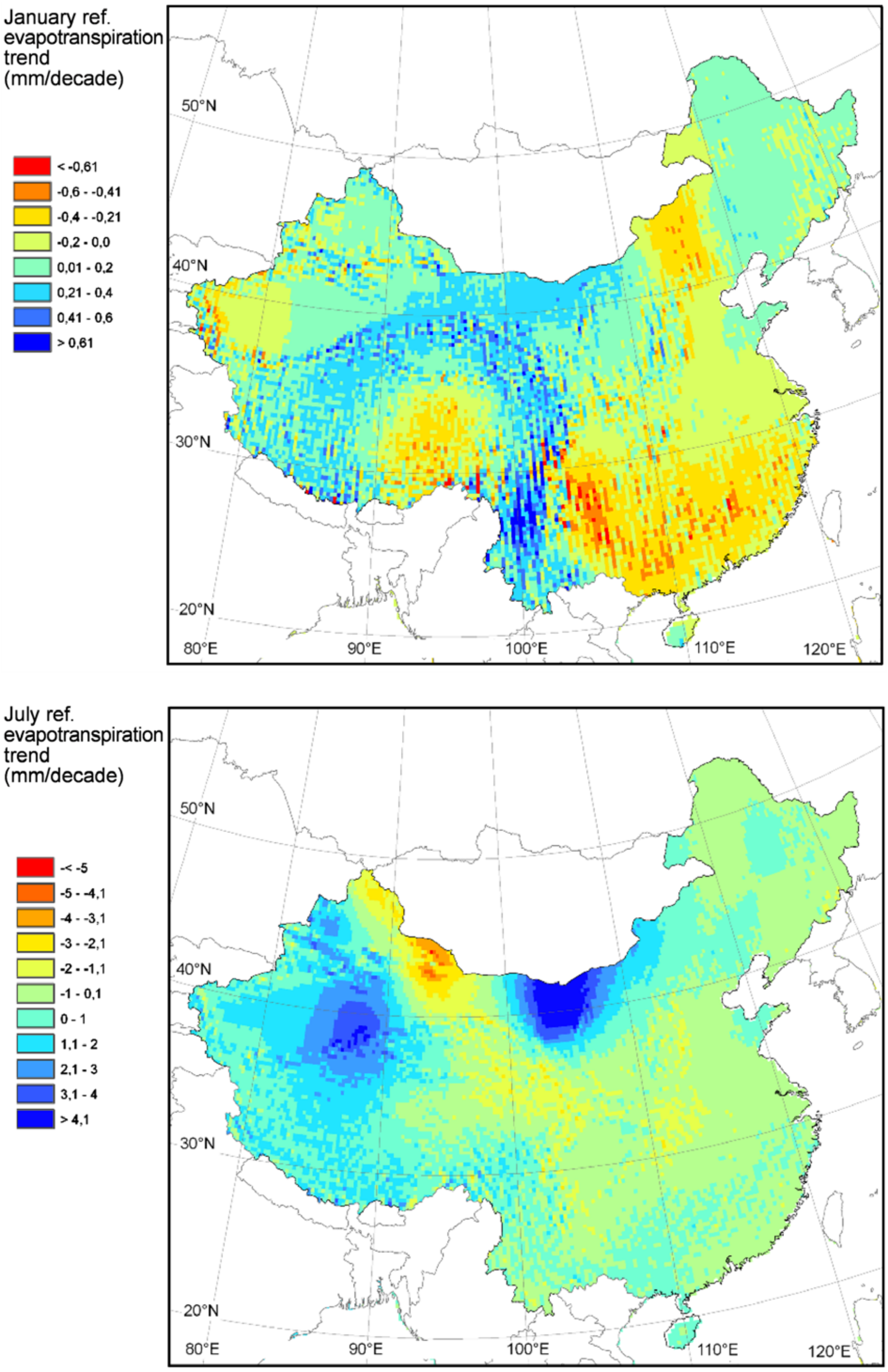

Figure 5 January (top) and July (bottom) Penman–Monteith reference evapotranspiration trend (1961–1990).

of the Yangtze and Mekong rivers on the eastern Tibetan Plateau. In the region of the annual *P* maximum along the Southeast Chinese coast runoff fraction reaches only values ~0.5.

Discussion

Annual ET0 rates in China (550–2300 mm) show a range comparable to annual *P* (15–2800 mm). No simple relationship exists between annual *P* and ET0 which might be inferred from the fact that low temperatures, high humidity and reduced sunshine duration associated with *P* should constrain ET0 rates. The same applies to a potential positive relationship between temperature and ET0.

In the summer months hot and windy conditions persist in the western parts of China when maximum monthly rates in the Taklamakan desert basin and the Tenger desert (see Fig. 1) reach about 400 mm. In both cases high insolation together with strong winds and high saturation deficit leads to the observed rates (Thomas, 2000). A particularly notewor-

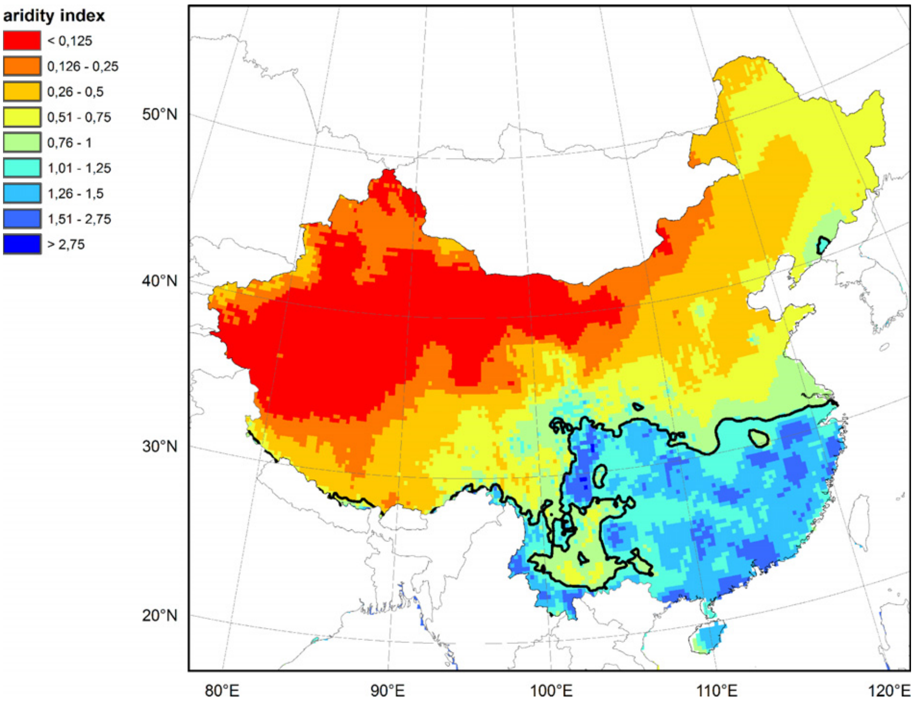

Figure 6 Aridity Index, calculated from long-term monthly average (1961—1990) data. The dark line marks AI = 1 calculated from long-term monthly average (1951—1980) data. Rivers have been omitted for clarity.

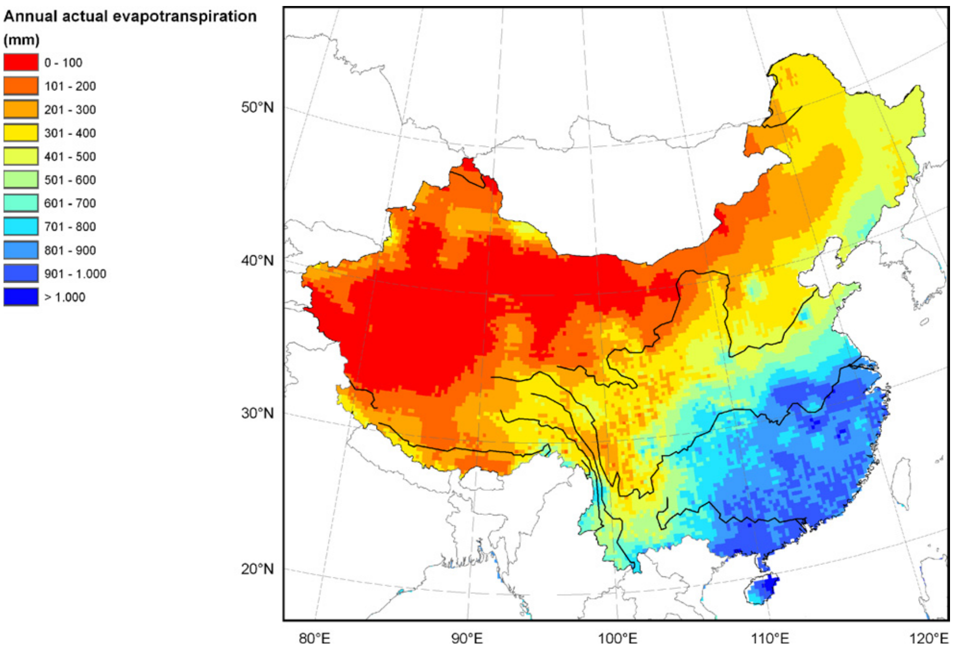

Figure 7 Annual actual evapotranspiration, calculated from long-term monthly average (1961—1990) data.

thy feature is increased ET0 along the south-exposed slopes of the eastern Tian Shan range. Local föhn winds descending the mountains lead to an extremely hot, dry and windy environment that culminates in the Turpan depression recording the highest ET0 rates in China. This well known climatic feature (Ren et al., 1985) is reproduced by the REGEOTOP procedure lending credibility to its regionalization ability to properly reflect topography-related climatic variations.

In contrast the lowest annual rates (~550 mm) are observed in the Sichuan basin where the lowest sunshine duration in China is recorded (Zhang and Lin, 1992) in addition to a constantly high water vapor content.

In winter the meridional decrease of ET0 rates from the south to the north illustrates the importance of solar inclination and day length. In the extremely cold northern parts of China ET0 rates drop to a few millimeters per month. A

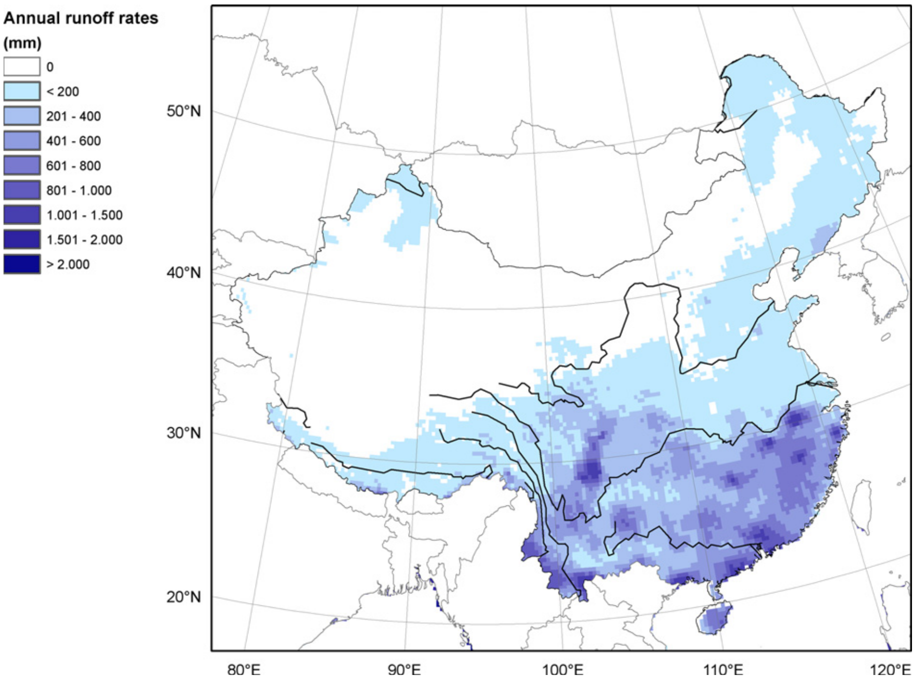

Figure 8 Annual runoff rates, calculated from long-term monthly average (1961—1990) data.

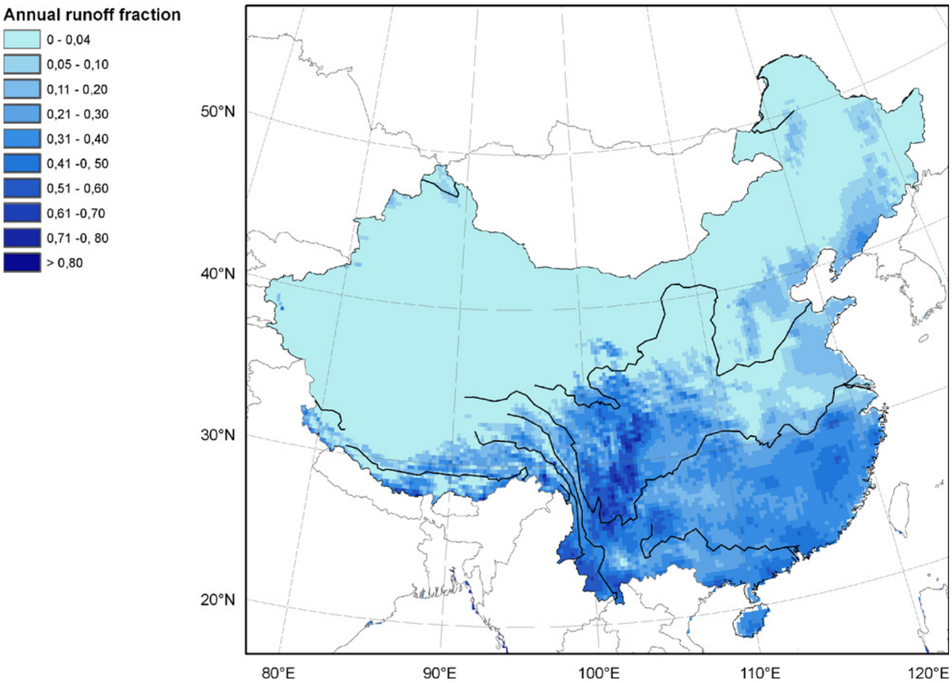

Figure 9 Annual runoff fraction, calculated from long-term monthly average (1961—1990) data.

snow cover can be observed north of 40°—45°N in at least 25 days while in the extreme northeastern and northwestern parts of China as well as in the northeastern part of the Tibetan Plateau snow cover exceeds three months (Zhang and Lin, 1992). As the basic assumptions of the reference surface of the PM equation are violated under these conditions estimated ET0 rates can only serve as a rough estimate. Under similar climatic conditions over snow covered glaciers in Northeast Greenland Soegaard et al., 2001 found ET rates of <0.2 mm/day (max. 1.7 mm/day) comparable to values estimated for Northeast China. Winter ET0 rates of up to 50 mm/month as given by Gao et al. (2006) in this area appear much too high. On the southern Tibetan Plateau winter ET0 rates are higher than in northern China despite an elevation difference of about 4000 m. This can be attributed to the mass elevation effect (Flohn, 1968) which leads to increased temperatures on high-altitude land surfaces compared to the free atmosphere at the same altitude.

In winter considerable differences in ET rates occur with highest ET0 rates in China observed in the mountainous southwestern provinces. In contrast to southeastern China which experiences cold and cloudy conditions under the continental branch of the winter monsoon southwestern China is located west of the 'Kunming quasi-stationary front' (located at ∼105°E) where cloudless and warm conditions persist under dry southwesterly air masses (Zhang, 1988). High elevation mountains and basins receive strong solar radiation while lowlands are blanketed by fog due to temperature inversions (Nomoto et al., 1988) leading to ET inversions with high ET rates above the clouds (Thomas, 2002). As a consequence no generalized elevational gradient for China as a whole can be given in winter as regional inversions lead to considerable scatter of winter ET0 rates (Fig. 10).

In summer the monsoon cloud cover leads to the lowest insolation rates and saturation deficits in China (Zhang and Lin, 1992) south of ∼35°N which in turn translates into monthly ET0 rates as low as 30 mm at elevations between 500–1500 m. ET0 rates of similar magnitude are also observed on the Tibetan Plateau above 4000 m where, despite low temperatures and elevation related decrease of saturation deficit, intense sunshine leads to comparable ET rates. Similar to winter conditions differences in elevation do not necessarily lead to differences in ET rates. As both southwest and southeast monsoonal air masses exhibit similar properties in summer ET0 rates on both sides of the quasi-stationary front are almost identical.

In response to the two circulation branches of the Asian monsoon system the seasonal distribution of ET0 rates varies strongly over the year. Comparing July to January ET0 rates (Fig. 11) shows that in the mountains of southwest China, southeastern Tibet and the Himalayas ET0 rates in January are comparable or may even surpass July rates. High January/July ET0 ratios are however not restricted to high elevations but occur also in deeply incised river valleys of the region. In regions where monsoonal cloud cover reduces ET0 rates during the peak monsoon months the annual ET0 maximum occurs out of phase with *P* in spring or early summer 2–3 months before the maximum of the monsoon rains. In addition ET0 tends to be more evenly spread over the year while *P* often exhibits a sharply defined rainy season of about four months duration from May to September. Hickel and Zhang (2006) and Potter et al. (2005) have shown that phase differences in the interannual variation of PET and *P* regimes may have a pronounced effect on the skill of hydrological models. This implies that hydrological studies that do not consider these out-of-phase effects may contain considerable errors.

Koster and Suarez (1999) assume that interannual variations of ET are in general smaller than those of *P*. Analysing PET estimates from GCM simulation Arora (2002) finds that when *P* variability is small PET variability may be similar in magnitude. In China variability of ET0 rates may reach those of *P* during the rainy season months. Increasing variability with elevation is observed both in summer and winter and is in agreement with Barry (1992) that PET in mountains is one of the most variable climatic elements. The assumed low PET variability may also be an artefact of temperature-based ET estimates that fail to physically capture variability that occurs through rapidly varying cloudiness and wind conditions that drive the process of evaporation.

Linear PET trend values are calculated based on the assumption of a gradual change over time. In reality however ET0 time series in China show considerable variations over time (Chen et al., 2006; Thomas, 2000). This implies that cited trend values depend on the arbitrary begin and end of the time series. Despite this shortcoming the large scale organization of trends appears to reflect the seasonal dynamics of the East Asian monsoon circulation. Particularly the demarcation between positive and negative trends along the 'Kunming quasi-stationary front' in winter points to the influence of air masses of different origin and contrasting physical properties on trend distribution. As sunshine duration (and hence cloudiness) and wind speeds govern most of the observed trends (Chen et al., 2006; Gong et al., 2006; Thomas, 2000) this implies changes in the

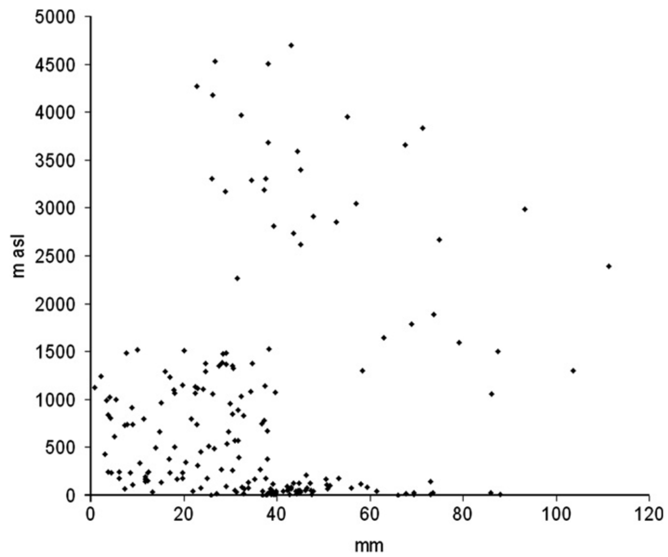

Figure 10 Mean monthly January ET0 rates (1961–1990) vs. station elevation for 196 meteorological stations in China.

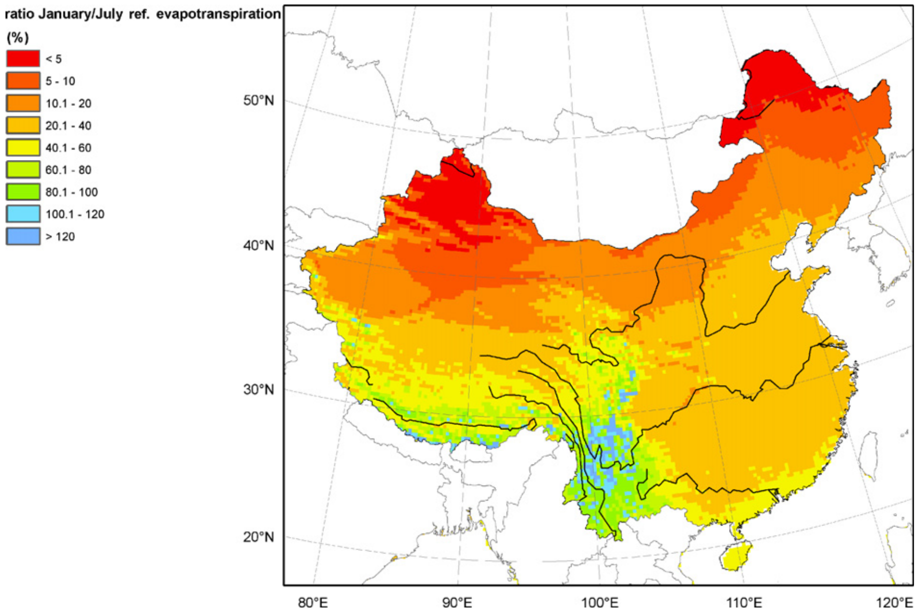

Figure 11 Ratio of mean monthly July to January Penman—Monteith reference evapotranspiration (1961—1990).

properties of the air masses or the circulation intensity of either the Southwest or Southeast monsoon (or both) as observed by Xu et al. (2006). Changes in wind speed appear to have considerable effect on ET rates not only in China but also in Australia (Rayner, 2007; Roderick et al., 2007) and on oceanic evaporation rates (Yu, 2007). During 1961—1990 this, however, appears not to have had a noticeable impact on runoff characteristics in the hydrologically sensitive region where the headwaters of major Asian rivers are located. In contrast AI in western Tibet at the upper reaches of the Indus appears to have increased from AI < 0.125 (extremely arid) to AI = 0.75—1 (semi-humid) which may be related to increases in P reported by Treydte et al. (2000). Additional data are required to evaluate temporal changes in detail as the reliability of the REGEOTOP grids in this region is low due to poor temporal and spatial coverage of contributing meteorological networks.

Additional data will also be needed at the border to Mongolia where maximum July trends of >4 mm/decade appear considerable too high in comparison to other regions with strong positive trends. Even though McVicar et al. (2005) found similar values for this region an inspection of individual times series derived from the corresponding pixel locations reveals a strongly irregular interannual variation that is not properly captured by a linear regression. While the cause of these fluctuations is unclear trend values in this region should be treated with extreme caution.

It should be noted that ET_a as defined in this context does not include the effects of vegetation, soil water storage, snow accumulation and melt on ET rates and does not represent ET_a in the strict sense as used by Doorenbos and Kassam (1986). With a wide range of different land uses and hence different ET rates, from bare desert soils with maximum ET_a of about 30% ET0 and deep-rooted evergreen forests (~ 90% ET0) to intensive triple cropping areas (~120% ET0 for a mid-season rice crop), ET_a derived from a sophisticated water balance model is expected to vary by a much wider margin than shown in Fig. 7. Using detailed land use information to model improved ET_a estimates would also require gridded data with increased resolution to match the spatial heterogeneity of land use patterns found in China. Fig. 9 shows the first hints of resolving the deep river valleys of southwestern China. Spatially distributed hydrological modeling of these regions with pronounced topography therefore requires gridded data with a spatial resolution equal or better than REGEOTOP data (0.25°) in order to provide spatially resolved results. Increasing data resolution alone without taking topographical controls of climate into account will, however, not lead to the desired results.

Conclusion

This study described the properties of a gridded high resolution reference evapotranspiration data set for China and surrounding regions. It could be shown that a number of assumptions about the spatial and temporal characteristics of evapotranspiration are not valid and that in some respect evapotranspiration is nearly as variable as precipitation. The assumed low evapotranspiration variability may be attributed to temperature-based evapotranspiration estimates that only reproduce the low variability inherent to temperature and fail to account for the influence of other, more rapidly varying climatic influences that directly control evapotranspiration. As these assumptions often pose the bases of theoretical considerations for hydrological studies considerable errors may result. Even though this study dealt with the climatological and hydrological characteristics of an evapotranspiration data set of China it is assumed that many properties can be regarded as typical for an east-coast monsoon region and should be transferable to other monsoon regions such as East Africa, northeast Australia or the southeastern coast of the US. A global investigation into the spatial and temporal characteristics of evapotranspiration based on the Penman—Monteith approach appears to be necessary in order to gain a better understanding of its influence on hydrological processes. Gridded data calculated with interpolation procedures that fail to account for the effects of topography, however, will not to give reliable information in this respect even if they provide high resolution.

In a large number of publications evapotranspiration is calculated from hydrological budgets using catchment average precipitation and catchment runoff data. Evapotranspiration estimates from climatological data provide an independent check on the results of these models. Changes in the hydrological activity, thought to be related to global warming, have occurred over North America (Huntington, 2006). Over most of China, however, the spatial distribution of runoff appears to have remained fairly constant during 1951–1990 which stands in contrast to the anticipated increase in hydrological activity.

Acknowledgements

Part of this study was supported by grant Th635/1 by the German Research Foundation (DFG). I would like to thank Tim McVicar for his help in improving the manuscript.

References

Allen, R.G., Pereira, L.S., Raes, D., Smith, M., 1998. Crop evapotranspiration. FAO Irrigation and Drainage Paper 56.

Arora, V.K., 2002. The use of aridity index to assess climate change effect on annual runoff. Journal of Hydrology 26, 164–177.

Baker, C.B., 1999. Area averaged temperature time series for China, India and the United States. <http://lwf.ncdc.noaa.gov/oa/climate/online/doe/doe.html> (19.12.07.).

Barry, R.G., 1992. Mountain Weather and Climate. London, 402pp.

Bechini, L., Ducco, G., Donatelli, M., Stein, A., 2000. Modelling, interpolation and stochastic simulation in space and time of global solar radiation. Agriculture, Ecosystems and Environment 81, 29–42.

Brutsaert, W., Parlange, M.B., 1998. Hydrological cycle explains the evaporation paradox. Nature 396, 30.

Budyko, M.I., 1974. Climate and Life. Orlando, 508pp.

Buishand, T.A., 1982. The analysis of homogeneity of long-term rainfall records in the Netherlands. Koninklijk Nederlands Meteorologisch Instituut Scientific Report WR 81-7, 86–87.

Calanca, P., Roesch, A., Jasper, K., Wild, M., 2006. Global warming and the summertime evapotranspiration regime of the Alpine region. Climatic Change 79, 65–78.

Chen, D., Gao, G., Xu, C.-Y., Guo, J., Ren, G., 2005. Comparison of the Thornthwaite method and pan data with the standard Penman–Monteith estimates of reference evapotranspiration in China. Climate Research 28, 123–132.

Chen, S., Liu, Y., Thomas, A., 2006. Climatic change on the Tibetan Plateau: potential evapotranspiration trends from 1961–2000. Climatic Change 76, 291–319.

Döll, P., Kaspar, F., Lehner, B., 2003. A global hydrological model for deriving water availability. Journal of Hydrology 270, 105–134.

Donohue, R.J., Roderick, M.L., McVicar, T.R., 2007. On the importance of including vegetation dynamics in Budyko's hydrological model. Hydrology and Earth System Sciences 11, 983–995.

Doorenbos, J., Kassam, A.H., 1986. Yield response to water. FAO Irrigation and Drainage Paper 33.

Fliri, F., 1967. Über die klimatologische Bedeutung der Kondensationshöhe im Gebirge. Die Erde 98, 203–210 (in German).

Flohn, H., 1968. Contributions to a meteorology of the Tibetan Highlands. Atmospheric Science Papers 130. Ft. Collins, 68pp.

Gao, G., Chen, D., Ren, G., Chen, Y., Liao, Y., 2006. Spatial and temporal variations and controlling factors of potential evapotranspiration in China: 1956–2000. Journal of Geographical Sciences 16, 3–12.

Garcia, M., Raes, D., Allen, R., Herbas, C., 2004. Dynamics of reference evapotranspiration in the Bolivian highlands (Altiplano). Agricultural and Forest Meteorology 125, 67–82.

Golubev, V.S., Lawrimore, J.H., Groisman, P.Y., Speranskaya, N.A., Zhuravin, S.A., Menne, M.J., Peterson, T.C., Malone, R.W., 2001. Evaporation changes over the contiguous United States and the former USSR: a reassessment. Geophysical Research Letters 28, 2665–2668.

Gong, L., Xu, C.-Y., Chen, D., Halldin, S., 2006. Sensitivity of the Penman–Monteith reference evapotranspiration to key climatic variables in the Changjiang (Yangtze River) Basin. Journal of Hydrology 329, 620–629.

Hagg, W., Braun, L.N., Kuhn, M., Neesgard, T.I., 2007. Modelling of hydrological response to climate change in glacierized Central Asian catchments. Journal of Hydrology 332, 40–53.

Hickel, K., Zhang, L., 2006. Estimating the impact of rainfall seasonality on mean annual water balance using a top-down approach. Journal of Hydrology 331, 409–424.

Huntington, T.G., 2006. Evidence for intensification of the global water cycle: review and synthesis. Journal of Hydrology 319, 83–95.

IWMI (International Water Management Institute): World Water & Climate Atlas. <http://www.iwmi.cgiar.org/WAtlas/atlas.htm> (assessed 19.12. 2007.).

Jensen, M.E., Burman, R.D., Allen, R.G., 1990. Evaporation and irrigation water requirements. ASCE Manuals and Reports on Engineering Practices No.70.

Koster, R.D., Suarez, M.J., 1999. A simple framework for examining the interannual variability of land surface moisture fluxes. Journal of Climate 12, 1911–1917.

Legates, D.R., Mather, J.R., 1992. An evaluation of the average annual global water balance. Geographical Review 82, 253–267.

Legates, D.R., McCabe, G.J., 2005. A re-evaluation of the average annual global water balance. Physical Geography 26, 467–479.

Ma, Z., Fu, C., 2003. Interannual characteristics of the surface hydrological variables over the arid and semiarid areas of northern China. Global and Planetary Change 37, 189–200.

Mardikis, M.G., Kalivas, D.P., Kollias, V.J., 2005. Comparison of interpolation methods for the prediction of reference evapotranspiration – an application in Greece. Water Resources Management 19, 251–278.

McVicar, T.R., Li, L.T., Van Niel, T.G., Hutchinson, M.F., Mu, X.M., Liu, Z.H., 2005. Spatially Distributing 21 Years of Monthly Hydrometeorological Data in China: Spatio-Temporal Analysis of FAO-56 Crop Reference Evapotranspiration and Pan Evaporation in the Context of Climate Change. CSIRO Land and Water Technical Report 8/05, Canberra, Australia, 316pp.

McVicar, T.R., Van Niel, T.G., Li, L.T., Hutchinson, M.F., Mu, X.M., Liu, Z.H., 2007. Spatially distributing monthly reference evapotranspiration and pan evaporation considering topographic influences. Journal of Hydrology 338, 196–220.

Milly, P.C.D., 1994. Climate, interseasonal storage of soil water, and the annual water balance. Advances in Water Resources 17, 19–24.

Mitchell, J.M., 1966. Climatic change. World Meteorological Organisation Technical Note 79.

New, M., Lister, D., Hulme, M., Makin, I., 2002. A high-resolution data set of surface climate over global land areas. Climate Research 21, 1–25.

Nomoto, S., Yasunari, T., Du, M., 1988. A preliminary study on fog and cold air lake in Jinghong and Mengyang basins, Xishuangbanna. Climatological Notes 38, 167–180.

Ohmura, A., Wild, M., 2002. Climate change: is the hydrological cycle accelerating? Science 298, 1345–1346.

Peterson, T.C., Golubev, V.S., Groisman, P.Ya., 1995. Evaporation loosing its strength. Nature 377, 687–688.

Philips, D.L., Marks, D., 1996. Spatial uncertainty analysis: propagation of interpolation errors in spatially distributed models. Ecological Modelling 91, 213–229.

Potter, N.J., Zhang, L., Milly, P.C.D., McMahon, T.A., Jakeman, A.J., 2005. Effects of rainfall seasonality and soil moisture capacity on mean annual water balances for Australian catchments. Water Resources Research 41, W06007. doi:10.1029/2004WR00369.

Prieler, S., 1999. Temperature and precipitation variability in China – a gridded monthly time series from 1958–1988. IIASA Interim Report IR-99-074, International Institute for Applied Systems Analysis, Laxenburg, Austria.

Priestley, C.H.B., Taylor, R.J., 1972. On the assessment of surface heat flux and evaporation using large-scale parameters. Monthly Weather Review 100, 81–92.

Rayner, D.P., 2007. Wind run changes: the dominant factor affecting pan evaporation trends in Australia. Journal of Climate 20, 3379–3394.

Ren, M.E., Yang, R.Z., Bao, H.S., 1985. An outline of China's physical geography. Beijing, 471pp.

Roderick, M.L., Farquhar, G.D., 2002. The cause of decreased pan evaporation over the past 50 years. Science 298, 1410–1411.

Roderick, M.L., Rotstayn, L.D., Farquhar, G.D., Hobbins, M.T., 2007. On the attribution of changing pan evaporation. Geophysical Research Letters 34, L17403. doi:10.1029/2007GL03116.

Scueltus, H.R., 1969. Arbeitsweisen Klimatologie. Westermann, Braunschweig, Germany, 128pp (in German).

Soegaard, H., Hasholt, B., Friborg, T., Nordstroem, C., 2001. Surface energy and water balance in a high arctic environment in NE Greenland. Theoretical and Applied Climatology 70, 35–51.

Thomas, A., 2000. Spatial analysis of Penman–Monteith evapotranspiration trends over China. International Journal of Climatology 20, 381–396.

Thomas, A., 2002. Seasonal and spatial variation of evapotranspiration in the mountains of Southwest China. Mountain Research 20, 51–59.

Thomas, A., Herzfeld, U.C., 2004. REGEOTOP: New climatic data fields for East Asia based on localized relief information and geostatistical methods. International Journal of Climatology 24, 1283–1306.

Thornthwaite, C.W., 1948. An approach towards a rational classification of climate. Geographical Revue 38, 55–94.

Thornthwaite, C.W., 1951. The water balance in tropical climates. Bulletin of the American Meteorological Society 32, 166–173.

Treydte, K.S., Schleser, G.H., Helle, G., Frank, D.C., Winiger, M., Haug, G.H., Esper, J., 2000. The twentieth century was the wettest period in northern Pakistan over the past millennium. Nature 440, 1179–1182.

Vicente-Serrano, S.M., Lanjeri, S., López-Moreno, J.I., 2007. Comparison of different procedures to map reference evapotranspiration using geographical information systems and regression-based techniques. International Journal of Climatology 27, 1103–1118.

Walter, A., Keuler, K., Jacob, D., Knoche, R., Block, A., Kotlarski, S., Müller-Westermeier, G., Rechid, D., Ahrens, W., 2006. A high resolution reference data set of German wind velocity and comparison with regional climate model results. Meteorologische Zeitschrift 15, 585–596.

Xu, M., Chang C.-P., Fu C., Qi Y., Robock A., Robinson D., Zhang, H., 2006. Steady decline of east Asian monsoon winds, 1969–2000: evidence from direct ground measurements of wind speed. Journal of Geophysical Research – Atmospheres 111, D24111, 10.1029/2006JD007337.

Yu, L., 2007. Global variations in oceanic evaporation (1958–2005): the role of the changing wind speed. Journal of Climate 20, 76–5390.

Yue, T., Fan, Z., Liu, J., 2005. Changes of major terrestrial ecosystems in China since 1960. Global and Planetary Change 48, 287–302.

Yue, T., Fan, Z., Liu, J., 2007. Scenarios of land cover in China. Global and Planetary Change 55, 317–342.

Zhang, K., 1988. The climatic dividing line between SW and SE Monsoons and their differences in climatology and ecology in Yunnan Province of China. Climatological Notes 38, 157–166.

Zhang, J., Lin, Z., 1992. The Climate of China. New York, 376pp.

Zheng, D., 1996. The system of physico-geographical regions of the Qinghai- Xizang (Tibet) Plateau. Science in China (Series D) 39, pp. 410–417.